

# Cyclotron line models for the X-ray pulsar A0535+26

R. A. Araya<sup>1</sup> and A. K. Harding<sup>2</sup>

<sup>1</sup> Department of Physics and Astronomy, Johns Hopkins University, Baltimore, MD 21218

<sup>2</sup> Laboratory for High Energy Astrophysics, NASA/Goddard Space Flight Center, Greenbelt, MD 20771

Received ; accepted

**Abstract.** The spectrum of the transient X-ray binary pulsar A0535+26 obtained by OSSE in February 1994 shows an absorption feature at 110 keV but does not confirm a feature at around 55 keV, as previously reported by other instruments. If the 110 keV feature is due to cyclotron scattering at the first harmonic, then the magnetic field required is about  $10^{13}$  Gauss, the highest observed in an X-ray pulsar. Conversely, if this strong feature is a second harmonic and the line formation process is such that an extremely weak fundamental results at  $\simeq 55$  keV, the estimate of the field strength is halved. We present results of detailed cyclotron line transfer models from two source geometries to explore the theoretical constraints on the line shapes in this source. It is found that while a fundamental harmonic line at  $\sim 55$  keV may be partially filled-in by angle redistribution in cylindrical geometries, the required viewing angles give a second harmonic line shape inconsistent with the observation. Interpretation of the feature at 110 keV as a first harmonic seen at small angles to the field yields more consistent line shapes.

**Key words:** X-rays: stars – Stars: neutron – Line formation – Radiation transfer

## 1. Introduction

Cyclotron line features have been detected in a number of X-ray pulsar spectra (Nagase 1989) and possibly also in the spectra of several gamma-ray bursts (Murakami et al. 1988). The line energies fall in the range from about 4 to 40 keV, indicating scattering of electrons in magnetic fields up to  $3.5 \times 10^{12}$  G. Detection of cyclotron scattering lines in spectra of astrophysical sources is extremely important because it is at present the only *direct* method for measuring the magnetic field of a neutron star.

The spectrum of the transient X-ray binary pulsar A0535+26 appears to show cyclotron features at the

highest energies yet measured from any source. The HEXE/TTM instrument on Mir/Kvant fit the spectrum observed from a 1989 outburst with two harmonic features at around 50 and 100 keV (Kendziorra et al. 1994). While the 100 keV feature reached  $5-6\sigma$  significance in some pulse phase intervals, the 50 keV feature was of very low ( $< 3\sigma$ ) significance. The OSSE instrument on CGRO observed a later outburst in 1994 and detected a highly significant ( $P < 10^{-15}$ ) feature in the phase averaged spectrum at 110 keV (no phase resolved spectra are yet available), but no feature at 50-55 keV (Grove et al. 1995). The present observations alone cannot determine whether the magnetic field in the source region is  $B \sim 5 \times 10^{12}$  G (5 TG), where the first cyclotron harmonic occurs at 55 keV, or  $B \sim 10^{13}$  G (10 TG), where the first harmonic is at 110 keV. This situation raises an important theoretical question: is it possible for some combination of physical parameters and source geometry to produce a strong second harmonic and a very weak or *undetectable* first harmonic?

In the present work, the parameter space of a relativistic resonant scattering simulation is sampled to model the conditions leading to the formation of the spectrum in A0535+26, for both low-field ( $B \simeq 5$  TG) and high-field ( $B \simeq 11$  TG) cases. In the low-field cases, the sensitivity of the line features to viewing angle with respect to the field allows a partial filling of the fundamental harmonic by photon redistribution. This effect along with the possible contribution of spawned photons from higher Landau levels are studied in detail. In the high-field case, there is no harmonic feature at 55 keV and the 110 keV absorption line is direct evidence for a magnetic field near the quantum critical field  $B_{cr} = m^2 c^3 / e\hbar = 44.13$  TG.

Resonant cyclotron features result from scattering of an incident photon spectrum by electrons in a magnetized plasma. The discreteness of electronic energy levels in a uniform magnetic field produces harmonic features in the emergent spectra which are highly sensitive to viewing angle with respect to the field and plasma geometry. As the ratio ( $B/B_{cr}$ ) nears 1, the study of strongly magnetized systems motivates a relativistic approach to the relevant

processes for the formation of cyclotron lines. To model the spectra of A0535+26, we use a Monte Carlo resonant transfer code which includes relativistic Quantum Electrodynamic magnetic cross sections allowing for the inclusion of up to four harmonics, photon spawning and angle redistribution of photons. In the following section we give a brief description of the code; a detailed account will be given elsewhere. Then, a report on trial runs to assess the likelihood of a low field *versus* a high field scenario is presented. More detailed fits, along with quantitative estimates for the goodness of the fits, are reported in Araya & Harding (1996).

## 2. Monte Carlo Resonant Transfer Code

The Monte Carlo code allows for the injection of individual photons and their diffusion in 3-D optical depth space. Relativistic treatment of cyclotron scattering is required when the magnetic field involved becomes comparable with  $B_{\text{cr}}$ . Our code uses the cyclotron scattering cross section calculated as a 2nd order QED process. Natural line widths of the cross sections are introduced via radiative corrections to the electron propagator, using solutions to the Dirac-Landau equation which diagonalize the self-interaction (Herold, Ruder & Wunner 1982). The corrections to the propagator introduce small imaginary terms in the resonant denominators, the lowest order being the cyclotron decay rate (Graziani, Harding & Sina 1995), resulting in a quasi-Lorentzian line shape. This prescription is used in our code for the scattering mean-free paths. A Lorentzian line width (absorption approximation: Harding & Daugherty 1991) is used to obtain the momentum of the scattering electron from the line profiles.

Furthermore, the code assumes a relativistic Maxwellian electron distribution function and includes excitation of higher Landau levels and the resultant photon spawning through cyclotron decay of these levels. Also, an approximate relativistic scattering angle redistribution of photons is used in place of the full differential cross section.

## 3. Model Calculations

We consider two geometries for the scattering region: plane slab, with the magnetic field parallel to the slab normal, and cylindrical, with the magnetic field parallel to the cylinder axis. An isotropic continuum photon spectrum is incident from a source at the slab midplane or along the cylinder axis. The escaping photons are accumulated in four ranges of  $\mu$ , the cosine of the viewing angle to the field. Following Grove et al. (1994), the continuum spectrum is modeled as a power law times an exponential:  $dN_\omega/(d\omega d\mu) \sim \omega^{-\alpha} \exp(-\omega/kT_c)$ , where  $\omega$  is the photon energy,  $\alpha$  is the power law index and  $T_c$  the continuum temperature. Due to the steepness of the input spectrum, the photons are injected with a flat spectral

distribution, and are assigned appropriate weight factors. This improves the statistics, but upscattered photons with large weight factors create some noise level in the high energy part of the spectrum. The line parameters are: the electron temperature  $T_e$ , the local magnetic field  $B$  (assumed uniform) and the minimum value of continuum optical depth  $\tau_c$  (in the direction parallel to  $B$  for a slab and perpendicular to  $B$  for a cylinder).

A discussion on the variation in the line shapes with different combination of parameters is given below but first we draw attention to the effect of multiple scatterings on the line features and thus, on our selection of parameters. Multiple scattering occurs mostly for first harmonic photons; higher harmonic photons are more likely to undergo single resonant Raman scattering, leaving the electron in an excited Landau level. Subsequent decay of these states produces spawned photons that, in essence, amounts to additional photon injection shortward of the fundamental energy (i.e. due to the anharmonic spacing of relativistic resonant energies). As  $B$  approaches  $B_{\text{cr}}$  multiple scattering becomes increasingly more important for higher harmonics. The line profiles are narrower and deeper at large angles and broader and shallower at small angles due in part to one-dimensional Doppler broadening. Thus, in a cylindrical scattering region, the lines are deepest at small angles, where the optical depth is largest:  $\tau_c^{cy}(\theta) = \tau_c/\sin\theta$ ; while in the slab geometry the lines are deepest at large angles, where outgoing photons encounter the largest optical depth:  $\tau_c^{sl}(\theta) = \tau_c/\cos\theta$  (compare Figs 2d and 2a). Thus, spawned photons and angle redistribution of photons through multiple scattering produce complex structure in the emerging fundamental line features. This influences the determination of model parameters in several ways. First, the inferred (from observation) hardness of the continuum may be strongly affected by broad line wings. Ideally, the fitting of three ‘uncontaminated’ continuum flux points would determine  $\alpha$  and  $T_c$ . However, for the particular case of the OSSE observation, choosing the third flux point on the blue side of the 110 keV line may violate this condition (see Fig. 2e). Second, although the resonances occur at well defined energies ( $\omega_{\text{res}}^n/m_e = [(1 + 2 n b \sin^2\theta)^{1/2} - 1]/\sin^2\theta$ ; where  $b \equiv B/B_{\text{cr}}$ ), the structure in the line introduces a larger uncertainty in the evaluation of the field strength than does the assumed viewing angle.

Third, the electron temperature cannot be easily estimated from the line widths. An estimate of the equilibrium electron temperature for A0535+26 can be found from the expression  $T_e = \omega_{\text{cyc}}/(2 + \alpha_{\text{eff}})$  of Lamb, Wang and Wasserman (1990), which is valid in the limit of a single scattering. In this approximation, the effective spectral indices of the continuum at the fundamental,  $\alpha_{\text{eff}} \sim 6.5$  and 3.6, yield  $T_e \simeq 12.9$  keV and 9.8 keV for the high and low field model electron temperatures respectively. However, in our modeling  $T_e$  must be considered a free parameter determined from the ‘symmetry’ of the resulting

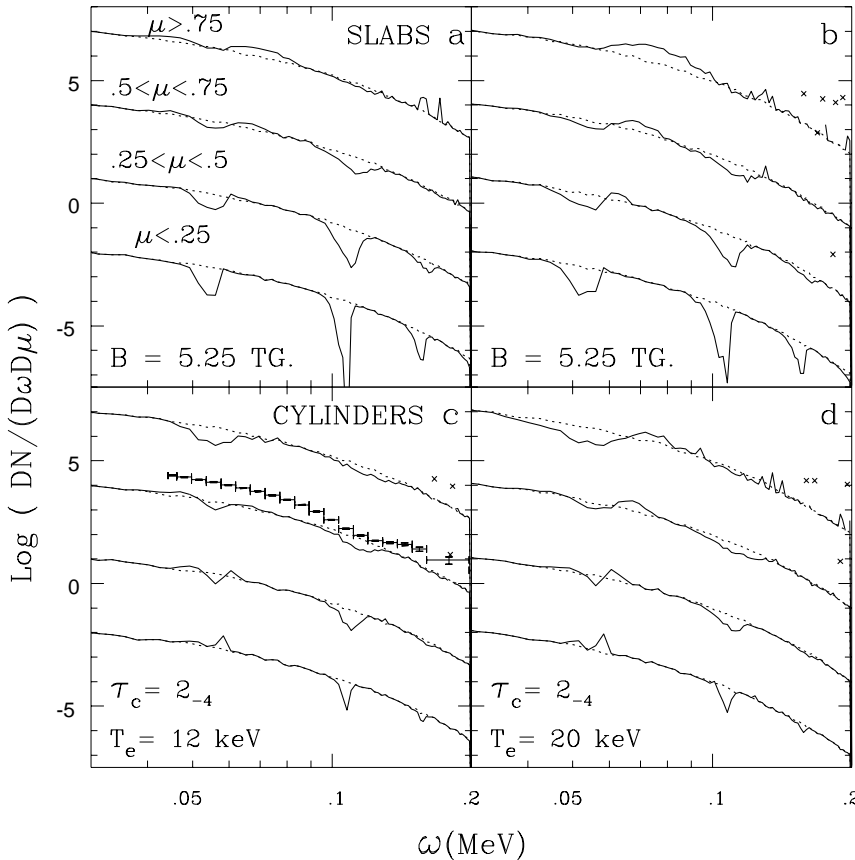


**Fig. 1.** Angle dependent model photon spectra for the lower field runs. Each run results from 50 to 100 thousand photons injected isotropically.  $\mu = \cos\theta$ . **Dotted line:** injected continuum. **Solid line:** output scattered spectrum. **Crosses:** single upscattered photons. **Horizontal error bars:** OSSE A0535+26 spectrum. Spectra from slabs are on the top and from cylinders on the bottom. Columns share the values of  $\tau_c$ ,  $T_e$ ,  $T_c$ ,  $\alpha$  and  $B$ .  $T_c = 14.5$  keV and  $\alpha = 0$  for all four runs. See text for notation. The flux normalization is arbitrary. These are local spectra emitted near the neutron star surface and do not include General relativistic effects such as red shift and light bending.

line shapes. Empirically we observe that too large a temperature results in blue excess emission mostly at small angles (Fig: 2c and 2f); on the other hand if  $T_e$  is too low, red excess emission is produced (Fig: 2a and 2d).

### 3.1. The Lower Field Case

Lower field models, shown in Fig 1, have  $B/B_{\text{cr}} \sim .12$ ,  $\omega_{\text{res}}(\mu = 0) = 57.5$  keV, and are constrained here so that either very narrow or very shallow first harmonics result (i.e. small equivalent width). Although spawned photons may produce additional injection around the fundamental energy, the steepness of the continuum in A0535+26 makes this process ineffective. For example, in the model shown in Fig 1c, spawned photons contribute only  $\sim 1\%$  of the flux at the first harmonic for  $.5 < \mu < .75$ . Nevertheless, ‘filling in’ at the fundamental energy may be attained in a cylindrical geometry, at a large viewing angle, through scattered photons from smaller angles (Figs 1c and 1d). Photons trapped close to the line center for  $\mu \sim 1$  escape more easily when scattered into  $\mu \sim 0$  where the line profiles are narrowest. However, for  $\mu \simeq 0$ , this re-

sults in measurable *emission* at the fundamental energy. Moreover, the resulting line widths at 110 keV are too narrow when compared to the data and increasing  $T_e$  (Fig. 1c) does not widen the second harmonic noticeably. For a slab, the effect of an overly high  $T_e$  is much more pronounced (Fig. 1d). Note that both geometries yield a very shallow fundamental feature for the angle bin  $.5 < \mu < .75$  (Figs. 1a and 1c) and a wide second harmonic feature for a reasonable temperature:  $T_e \sim 12$  keV. Nevertheless, the feature at the fundamental energy is at least half the depth of the second harmonic, and would have been clearly identifiable by the OSSE observations (shown with error bars in Fig 1c) as it spans about two energy bins of the OSSE instrument.

### 3.2. The Higher Field Case

In our high field models,  $B/B_{\text{cr}} \sim .21 - .25$  and  $\omega_{\text{res}}^1(\mu = 1) = 120 - 129$  keV. We find the parameters of the scattering region which are best able to produce a first harmonic feature similar to the observed line at 110 keV. When account is made for the structure in the line, fields as high as 11 TG may be consistent with the observed line. Fig 2 exhibits a sample of high field model spectra, and illustrates that the closest line feature to that of A0535+26 is provided by a cylindrical geometry (Fig. 2e) and for angle

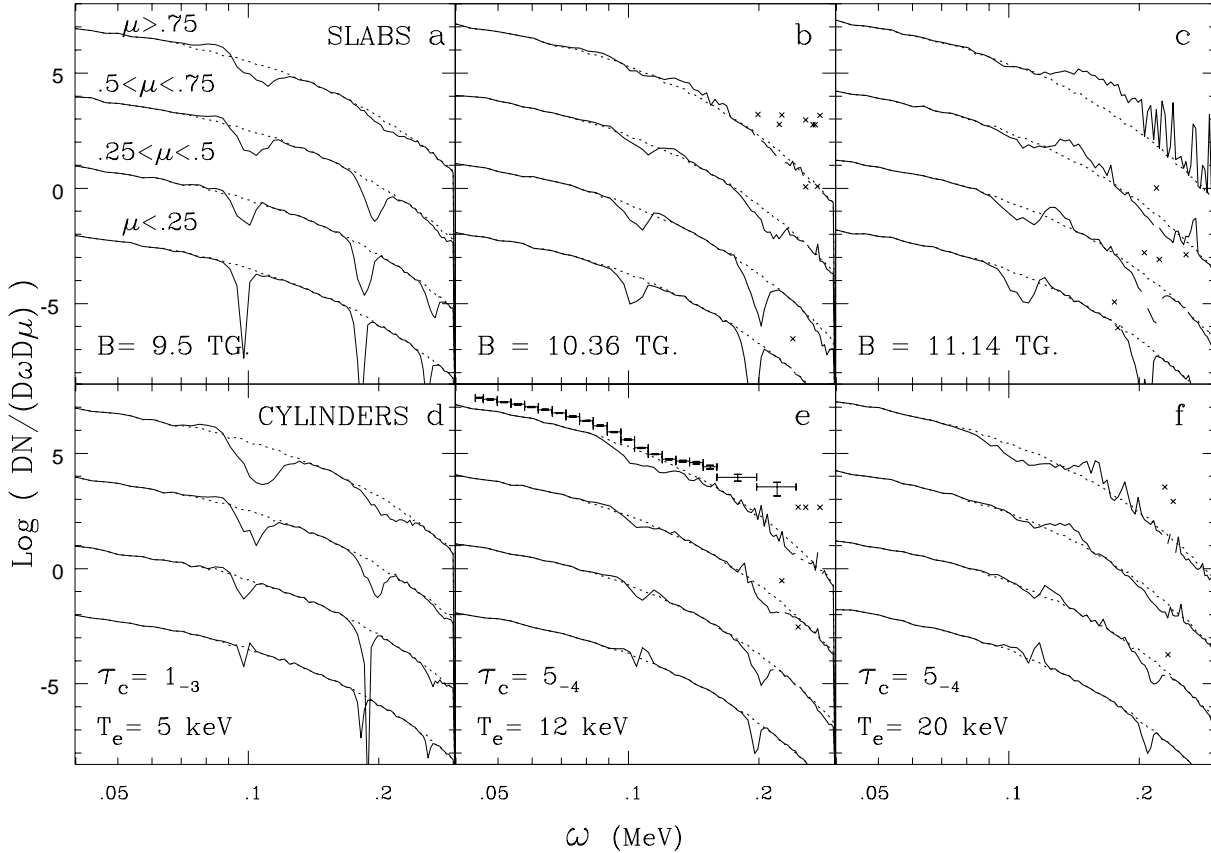


**Fig. 2.** Angle dependent model photon spectra for higher field cases.  $T_c = 17.8$  keV and  $\alpha = -0.13$  for the two leftmost spectra and 14.5 keV and 0 for the rest. Error bars are the A0535+26 data.

bin  $.75 < \mu < 1$ . The model has three free parameters:  $B$ ,  $\tau_c$  and  $T_e$ .

#### 4. Conclusions

Based on our theoretical models of the spectrum of A0535+26, assuming both low and high magnetic fields and a range of electron temperature, optical depth and continuum spectrum shape, we conclude that the observed 110 keV feature is more likely to be a first harmonic. Our conclusion is, however, limited by the fact that we have thus far made only qualitatively comparisons between our model spectra and the OSSE photon spectrum. The latter has already assumed a particular line and continuum shape to unfold the observed count spectrum. Given that escape of cyclotron photons into the line wings can significantly affect the surrounding continuum, it is important to fit both the line and continuum spectrum simultaneously. We are planning to carry out formal fits to both the OSSE and HEXE/TTM phase-resolved spectra, folding our model spectra through the response functions of the detectors. It will then be possible to make a more

quantitative statement about the likelihood of a high field ( $B \sim 10$  TG) vs. a low field ( $B \sim 5$  TG) in A0535+26.

*Acknowledgements.* We thank Dr. Ramin Sina for aid in the scattering cross section code and Dr. Alexander Szalay for allowing us access to speedy computer resources at the Johns Hopkins University.

#### References

- Araya, R. A. & Harding, A. K., 1996, ApJ, 463, L33.
- Graziani, C., Harding, A.K. & Sina, R., 1995, Phys.Rev.D, 51, 7097.
- Grove, J.E. et al., 1995, Ap.J., 438, L25 .
- Harding, A.K. & Daugherty, J.K., 1991, Ap.J., 374, 687.
- Herold, H., Ruder, H. & Wunner, G., 1982, Astron. Astrophys., 115, 90.
- Kendziorra, E. et al., 1994, A & A, 291, L31.
- Lamb, D.Q., Wang, J.C.L. & Wasserman, I.M., 1990, Ap.J., 363, 670.
- Murakami, T. et al., 1988, Nature, 335, 234.
- Nagase, F., 1989, Publ. Astron. Soc. Japan, 41, 1.

This article was processed by the author using Springer-Verlag L<sup>A</sup>T<sub>E</sub>X A&A style file *L-AA* version 3.